SIAM J. SCI. COMPUT.
Vol. 24, No. 3, pp. 955–978
© 2002 Society for Industrial and Applied Mathematics

A WAVE PROPAGATION METHOD FOR CONSERVATION LAWS AND BALANCE LAWS WITH SPATIALLY VARYING FLUX FUNCTIONS*

DEREK S. BALE†, RANDALL J. LEVEQUE†, SORIN MITRAN†, AND JAMES A. ROSSMANITH†

Abstract. We study a general approach to solving conservation laws of the form $q_t+f(q,x)_x=0$, where the flux function $f(q,x)$ has explicit spatial variation. Finite-volume methods are used in which the flux is discretized spatially, giving a function $f_i(q)$ over the ith grid cell and leading to a generalized Riemann problem between neighboring grid cells. A high-resolution wave-propagation algorithm is defined in which waves are based directly on a decomposition of flux differences $f_i(Q_i)-f_{i-1}(Q_{i-1})$ into eigenvectors of an approximate Jacobian matrix. This method is shown to be second-order accurate for smooth problems and allows the application of wave limiters to obtain sharp results on discontinuities. Balance laws $q_t+f(q,x)_x=\psi(q,x)$ are also considered, in which case the source term is used to modify the flux difference before performing the wave decomposition, and an additional term is derived that must also be included to obtain full accuracy. This method is particularly useful for quasi-steady problems close to steady state.

Key words. finite-volume methods, high-resolution methods, conservation laws, source terms, discontinuous flux functions

AMS subject classifications. 65M06, 35L65

PII. S106482750139738X

1. Introduction.

Our goal is to develop high-resolution finite-volume methods for hyperbolic conservation laws with spatially varying flux functions. In one space dimension such an equation has the form

$$q_t + f(q,x)_x = 0, \tag{1.1}$$

where $q(x,t)\in\mathbb{R}^m$ is the vector of conserved quantities and $f:\mathbb{R}^m\times\mathbb{R}\to\mathbb{R}^m$ is the flux function, possibly a nonlinear function of q. We also consider balance laws where the right-hand side of (1.1) is replaced by a source term $\psi(q,x)$. Subscripts denote partial derivatives; note that $f(q,x)_x=\partial_x[f(q,x)]=f_q(q,x)q_x+f_x(q,x)$.

Problems with spatially varying flux functions arise in many applications, for example, traffic flow on roads with varying conditions, nonlinear elasticity in heterogeneous materials, or flow through heterogeneous porous media. Solving conservation laws on curved manifolds also leads to spatially varying flux functions, an application that is considered in a separate paper [2] and the recent theses [1] and [29]. Application to a problem in gravitational waves is discussed by Bardeen and Buchman [3].

Spatially varying flux functions lead to difficulties not seen in the autonomous case, some of which are discussed below. In this paper we concentrate on the case in which the eigenvalues of the flux Jacobian $f_q(q,x)$ do not pass through zero, so that

*Received by the editors November 2, 2001; accepted for publication (in revised form) June 2, 2002; published electronically December 19, 2002. This work was supported in part by DOE grant DE-FG03-00ER2592 and NSF grants DMS-9803442 and DMS-0106511.
http://www.siam.org/journals/sisc/24-3/39738.html
†Department of Applied Mathematics, University of Washington, Box 352420, Seattle, WA 98195-2420 (dbale@amath.washington.edu, rjl@amath.washington.edu, mitran@amath.washington.edu, jrossman@amath.washington.edu).

there are a fixed number of positive eigenvalues. The reasons for this assumption are discussed in section 2.

The *autonomous* case

$$q_t + f(q)_x = 0, \tag{1.2}$$

where f depends only on q, has been studied extensively, and a variety of numerical methods have been developed. We concentrate on extending the high-resolution wave-propagation algorithms of [20] to the case of a spatially varying flux function. These are finite-volume methods in which a cell average

$$Q_i^n \approx \frac{1}{\Delta x} \int_{x_{i-1/2}}^{x_{i+1/2}} q(x, t_n)\, dx \tag{1.3}$$

is updated in each time step. This is done using the wave structure determined by solving Riemann problems at cell edges. They are higher-order Godunov methods in which wave limiters are used to suppress nonphysical oscillations. For an *autonomous* system the Riemann problem at $x_{i-1/2}$ consists of (1.2) with the piecewise constant initial data

$$q(x,0) = \begin{cases} Q_{i-1} & \text{if } x < x_{i-1/2}, \\ Q_i & \text{if } x > x_{i-1/2}. \end{cases} \tag{1.4}$$

The Riemann solution for an autonomous system of m equations typically consists of m waves that we denote by $\mathcal{W}_{i-1/2}^p$ for $p = 1, 2, \ldots, m$, propagating with speeds $s_{i-1/2}^p$. We assume that the waves are discontinuities in the solution (i.e., shocks or contact discontinuities) and that

$$Q_i - Q_{i-1} = \sum_{p=1}^{m} \mathcal{W}_{i-1/2}^p. \tag{1.5}$$

In the wave-propagation algorithms, both the first-order Godunov method and high-resolution correction terms are based on these waves and their speeds. A nonlinear problem may involve rarefaction waves as well, but in this case the Riemann solution is typically approximated by something of the above form, e.g., by using the Roe solver (see section 2) or some other local linearization of the problem.

We use $Q_{i-1/2}$ to denote the value of q along the line $x \equiv x_{i-1/2}$ in the Riemann solution. This value is used in implementing Godunov's method in flux-differencing form,

$$Q_i^{n+1} = Q_i^n - \frac{\Delta t}{\Delta x}(\mathcal{F}_{i+1/2} - \mathcal{F}_{i-1/2}), \tag{1.6}$$

where $\mathcal{F}_{i-1/2} = f(Q_{i-1/2})$ is the flux across the interface at $x_{i-1/2}$.

In the *spatially varying* case (1.1), the flux function $f(q, x)$ can be discretized with respect to x in some manner consistent with a finite-volume interpretation. For a given grid, two possible discretizations are natural to consider: cell-centered flux functions or edge-centered flux functions, as we now describe.

Cell-centered flux functions. In this approach we assume that the flux function $f(q, x)$ is discretized to yield a flux function $f_i(q)$ that holds throughout the ith grid cell. This is very natural for many problems. For an elasticity problem in a

heterogeneous rod, for example, we might assume that each grid cell is made up of a single material, and the flux $f_i(q)$ for this cell is then determined by the constitutive relations for this material. For traffic flow problems, each grid cell corresponds to a short stretch of highway over which the road conditions and speed limit are assumed to be constant, leading to a specific flux function valid in this cell. This flux function might be defined simply by $f_i(q) = f(q, x_i)$ if the variation of f with x is sufficiently smooth, or a more sophisticated homogenization procedure may be needed if f varies substantially on the subgrid scale. When cell-centered flux functions are used, the *generalized Riemann problem* at cell interface $x_{i-1/2}$ consists of the equation

$$q_t + F_{i-1/2}(q, x)_x = 0 \tag{1.7}$$

together with the initial data (1.4), where

$$F_{i-1/2}(q, x) = \begin{cases} f_{i-1}(q) & \text{if } x < x_{i-1/2}, \\ f_i(q) & \text{if } x > x_{i-1/2}. \end{cases} \tag{1.8}$$

The Riemann solution may be more complicated than in the autonomous case and is discussed in section 2.

Cell-edge flux functions. An alternative approach is to assume that a distinct flux function $f_{i-1/2}(q)$ is associated with each cell interface $x_{i-1/2}$. This is natural if we interpret the flux function as measuring the flow between cell $i-1$ and cell i. It is the flux at the cell interface that is ultimately required to implement a finite-volume method based on flux differencing, and so associating flux functions with interfaces often makes sense. We can relate this to the cell-centered flux approach by viewing the flux $f_{i-1/2}(q)$ as holding over the interval $[x_{i-1}, x_i]$ between the center of cell $i-1$ and the center of cell i. The Riemann problem at $x_{i-1/2}$ is now a classical Riemann problem for the single equation $q_t + f_{i-1/2}(q)_x = 0$ with the data (1.4). However, in order to implement the wave-propagation algorithm, it would also be necessary to consider a second set of Riemann problems at the cell centers x_i, where the flux function jumps. Nontrivial waves can arise from these points even though the data Q_i is the same on both sides.

In this paper we assume that cell-centered flux functions are specified. This is appropriate for many problems as discussed above. Our approach applies directly only to this case, since it is the flux difference between cells that is decomposed into waves. We develop an approach for approximately solving the generalized Riemann problem (1.7) at $x_{i-1/2}$ in an efficient manner that can be used in conjunction with a modified wave-propagation algorithm. This algorithm is based on an approximate Jacobian matrix $A_{i-1/2}$ that must be defined at the cell edge. A similar approach is frequently used for nonlinear autonomous problems where the fluxes $f(Q_{i-1})$ and $f(Q_i)$ are used to define an averaged Jacobian matrix $A_{i-1/2}$ (e.g., the Roe average). The original nonlinear Riemann problem is then replaced by the linear Riemann problem for the equation

$$q_t + A_{i-1/2} q_x = 0. \tag{1.9}$$

In fact we do not need the matrix $A_{i-1/2}$ itself but simply its eigenvalues $s^p_{i-1/2}$ and eigenvectors $r^p_{i-1/2}$ (for $p = 1, 2, \ldots, m$) since these are used directly in solving the Riemann problem. In the spatially varying case, various approaches to choosing these eigenvectors based on the neighboring fluxes are possible. One natural way is to choose the eigenvectors of $f'_{i-1}(Q_{i-1})$ that correspond to negative eigenvalues

(and hence left-going waves) and combine these with the eigenvectors of $f_i'(Q_i)$ that correspond to right-going waves. This is only possible if this yields a set of m linearly independent vectors, however, as discussed further in section 2.

The classical Riemann problem for the constant-coefficient system (1.9) with data (1.4) can be easily solved in terms of the eigenvectors $r^p_{i-1/2}$. The standard approach is to decompose the jump in Q as a linear combination of the eigenvectors in order to define waves $\mathcal{W}^p_{i-1/2}$:

$$Q_i - Q_{i-1} = \sum_{p=1}^{m} \alpha^p_{i-1/2} r^p_{i-1/2} \equiv \sum_{p=1}^{m} \mathcal{W}^p_{i-1/2}. \tag{1.10}$$

The coefficients $\alpha^p_{i-1/2}$ are given by

$$\alpha^p_{i-1/2} = R^{-1}_{i-1/2}(Q_i - Q_{i-1}), \tag{1.11}$$

where $R_{i-1/2}$ is the matrix of right eigenvectors. However, using these waves $\mathcal{W}^p_{i-1/2}$ in the wave-propagation algorithm of [20] (see section 3) will not yield a conservative algorithm in general, unless the condition

$$A_{i-1/2}(Q_i - Q_{i-1}) = f_i(Q_i) - f_{i-1}(Q_{i-1}) \tag{1.12}$$

happens to be satisfied. For an autonomous system ($f_i(q) \equiv f(q)$) this reduces to the condition imposed in defining the "Roe average" $A_{i-1/2}$ (see [27]), and considerable research has gone into defining averaged Jacobians with this property for specific nonlinear problems.

The main novel feature of the algorithm we present here is the following. We do not solve the Riemann problem by performing a classical decomposition of the form (1.10). Instead we use a *flux-based wave decomposition*, in which we directly decompose the flux difference $f_i(Q_i) - f_{i-1}(Q_{i-1})$ as a linear combination of the eigenvectors $r^p_{i-1/2}$,

$$f_i(Q_i) - f_{i-1}(Q_{i-1}) = \sum_{p=1}^{m} \beta^p_{i-1/2} r^p_{i-1/2} \equiv \sum_{p=1}^{m} \mathcal{Z}^p_{i-1/2}, \tag{1.13}$$

where

$$\beta_{i-1/2} = R^{-1}_{i-1/2}(f_i(Q_i) - f_{i-1}(Q_{i-1})). \tag{1.14}$$

For spatially varying fluxes this is a more natural decomposition for reasons discussed in section 2. This decomposition can also be related to a generalized relaxation scheme for the conservation law as discussed in [23]. The vectors $\mathcal{Z}^p = \beta^p r^p$ will be called f-waves, as they are analogous to the waves $\mathcal{W}^p$ from (1.10) but carry flux increments rather than increments in q.

A potential advantage of using the decomposition (1.13) instead of (1.10), even in the autonomous case, is that our resulting method is conservative even if (1.12) is not satisfied. This yields a more flexible algorithm for problems where a Roe average is not easily computed. To highlight the relation between this approach and the standard wave-propagation algorithm, note that if the matrix $A_{i-1/2}$ does in fact satisfy (1.12), then multiplying (1.10) by $A_{i-1/2}$ leads to

$$f_i(Q_i) - f_{i-1}(Q_{i-1}) = \sum_{p=1}^{m} \alpha^p_{i-1/2} s^p_{i-1/2} r^p_{i-1/2}, \tag{1.15}$$

since $r^p_{i-1/2}$ is an eigenvector of $A_{i-1/2}$. Hence if we define waves $\mathcal{W}^p_{i-1/2}$ by (1.10), then we can define f-waves by $\mathcal{Z}^p_{i-1/2} = s^p_{i-1/2}\mathcal{W}^p_{i-1/2}$ and obtain the same result as by performing the decomposition (1.13).

Dimensionally the f-waves have the form of a q increment multiplied by the wave speed. It is these quantities that are really needed in implementing Godunov's method and high-resolution versions, and in section 3 we show how the wave-propagation algorithm can be implemented directly in terms of these f-waves and the speeds s^p without needing the $\mathcal{W}^p$. We obtain a method that is second-order accurate on smooth solutions (if the flux function has smooth spatial variation) and to which wave limiters can be applied in order to obtain a high-resolution method that also captures discontinuities well.

For balance laws that include a source term,

$$q_t + f(q,x)_x = \psi(q,x), \tag{1.16}$$

we can easily extend this algorithm by first discretizing the source term to obtain values $\Psi_{i-1/2}$ at cell interfaces and then basing the algorithm on f-waves $\mathcal{Z}^p_{i-1/2}$ that are defined by decomposing

$$f_i(Q_i) - f_{i-1}(Q_{i-1}) - \Delta x \Psi_{i-1/2} = \sum_{p=1}^{m} \beta^p_{i-1/2} r^p_{i-1/2} \equiv \sum_{p=1}^{m} \mathcal{Z}^p_{i-1/2}, \tag{1.17}$$

i.e.,

$$\beta_{i-1/2} = R^{-1}_{i-1/2}(f_i(Q_i) - f_{i-1}(Q_{i-1}) - \Delta x \Psi_{i-1/2}). \tag{1.18}$$

This approach to handling source terms is useful even for autonomous problems, particularly in cases where the solution is close to a steady state in which the flux gradient should nearly balance the source term, since it is only the discrepancy between these that is decomposed into propagating waves. In particular, this seems to be a more robust approach than the quasi-steady wave-propagation algorithm proposed in [21], as noted in [23]. Full second-order accuracy can also be achieved with this approach, though it requires the addition of another correction term to the wave-propagation algorithm. This is discussed further in section 7.

Homogeneous systems of the form (1.1) with spatially varying flux functions can also have nontrivial steady state solutions in which $f(q,x)_x = 0$ but q is not identically constant. The f-wave approach has the advantage of capturing such steady states well and also accurately solving quasi-steady problems where the goal is to capture the propagation of small amplitude perturbations.

2. Solving the generalized Riemann problem. In this section we investigate the solution to the generalized Riemann problem given by (1.7) with data (1.4). We start by considering the simplest possible case, the advection equation

$$q_t + (u(x)q)_x = 0. \tag{2.1}$$

This is a scalar ($m = 1$) variable-coefficient linear problem with flux

$$f(q,x) = u(x)q. \tag{2.2}$$

We discretize this flux using the cell-centered flux functions $f_i(q) = u_i q$, where u_i is the advection velocity in the ith cell. This might model traffic flow on a one-lane

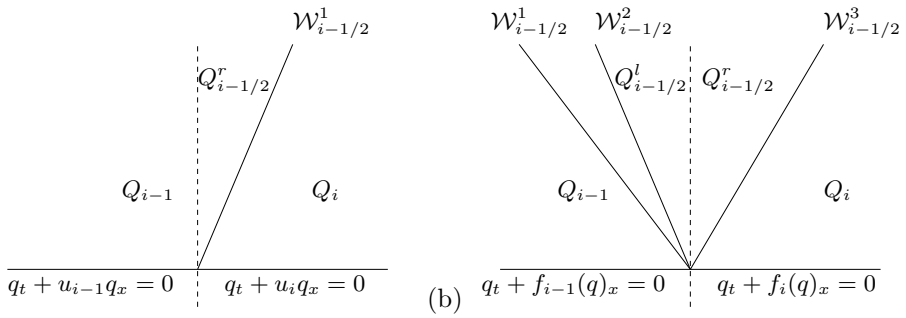

FIG. 1. (a) *Riemann solution for the variable-coefficient advection equation in the case* $u_{i-1} > 0$ *and* $u_i > 0$. (b) *Structure of the Riemann solution for a generalized Riemann problem with* $m = 3$.

road where drivers always drive at the speed limit $u(x)$ regardless of the density q. Then u_i would represent the speed limit over the stretch of road covered by the ith grid cell. For this application we would normally assume that u_i has the same sign everywhere, say $u_i > 0$. (Below we comment on what happens if this is not satisfied.) Then the Riemann solution is

$$q(x,t) = \begin{cases} Q_{i-1} & \text{if } x < x_{i-1/2}, \\ Q^r_{i-1/2} & \text{if } x_{i-1/2} < x < x_{i-1/2} + u_i t, \\ Q_i & \text{if } x > x_{i-1/2} + u_i t, \end{cases} \tag{2.3}$$

where

$$Q^r_{i-1/2} = \frac{u_{i-1} Q_{i-1}}{u_i} \tag{2.4}$$

is the value of q just to the right of $x_{i-1/2}$, as illustrated in Figure 1(a). There is a single propagating wave $\mathcal{W}^1_{i-1/2}$ with speed $s^1_{i-1/2} = u_i$, but note that there is also a stationary discontinuity in q at $x_{i-1/2}$ that arises from the jump in advection velocity at this point, which leads to a corresponding jump in the density of traffic. The flux, however, should be continuous at this point since all cars leaving cell $i-1$ must enter cell i. This requires $u_{i-1}Q_{i-1} = u_i Q^r_{i-1/2}$ and leads to the expression (2.4).

For a system of m equations, the generalized Riemann solution to (1.7) may have the structure indicated in Figure 1(b) for $m = 3$. Along with a set of propagating waves $\mathcal{W}^p_{i-1/2}$, there is also a jump in q at $x_{i-1/2}$, and we use $Q^l_{i-1/2}$ and $Q^r_{i-1/2}$ to denote the value of q just to the left and right of this point. Typically we expect the flux to be continuous at $x_{i-1/2}$ in the Riemann solution so that the flux out of cell $i-1$ agrees with the flux into cell i,

$$f_{i-1}(Q^l_{i-1/2}) = f_i(Q^r_{i-1/2}). \tag{2.5}$$

Note that this is a special case of the Rankine–Hugoniot jump condition across the stationary discontinuity at $x_{i-1/2}$.

For the scalar advection equation (2.1), $m = 1$ and we can choose $r^1_{i-1/2} = 1$ as the eigenvector of $A_{i-1/2}$ with eigenvalue $s^1_{i-1/2} = u_i$, so that $A_{i-1/2} = u_i$. Note that attempting to solve the Riemann problem by a decomposition of the form (1.10) would fail in this case, as it would lead to $\mathcal{W}^1_{i-1/2} = \alpha^1_{i-1/2} = Q_i - Q_{i-1}$, which is not correct. The problem is that we have neglected to take into account the jump in q at $x_{i-1/2}$.

If instead we use the decomposition (1.13), then we obtain the correct Riemann solution (2.3), since then $\mathcal{Z}^1_{i-1/2} = f_i(Q_i) - f_{i-1}(Q_{i-1}) = u_i Q_i - u_{i-1} Q_{i-1}$. This is correct since the entire flux difference is carried by the one propagating wave, with no flux difference remaining at $x_{i-1/2}$. Note that we can recover the correct wave $\mathcal{W}^1_{i-1/2}$ of Figure 1(a) from this by dividing $\mathcal{Z}^1_{i-1/2}$ by the wave speed (as suggested by comparing (1.15) and (1.10)),

$$\begin{aligned} \mathcal{W}^1_{i-1/2} &= \frac{\mathcal{Z}^1_{i-1/2}}{s^1_{i-1/2}} \\ &= \frac{(u_i Q_i - u_{i-1} Q_{i-1})}{u_i} \\ &= Q_i - Q^r_{i-1/2}, \end{aligned} \tag{2.6}$$

but in section 3 we will see that the f-wave $\mathcal{Z}^1_{i-1/2}$ can also be used directly in a wave-propagation algorithm.

This illustrates a primary advantage of the f-wave approach. Attempting to solve the generalized Riemann problem in terms of waves $\mathcal{W}^p$ as illustrated in Figure 1(b) requires also determining the proper jump $Q^r_{i-1/2} - Q^l_{i-1/2}$, since q is not continuous across $x_{i-1/2}$. We would need to determine waves $\mathcal{W}^p_{i-1/2}$ that are proportional to eigenvectors $r^p_{i-1/2}$ and that also lead to states $Q^r_{i-1/2}$ and $Q^l_{i-1/2}$ satisfying (2.5). In the nonlinear case this leads to a nonlinear system of equations to solve. By working instead in terms of the flux difference, the fact that the flux is continuous across $x_{i-1/2}$ works to our advantage since the entire flux difference can then be decomposed into propagating f-waves using the linear decomposition (1.13).

We must note, however, that this is true only for conservation laws that have bounded solutions for which the flux is continuous everywhere. Some conservation laws with spatially varying flux functions develop singularities in the form of delta functions at points where the flux $f(q, x)$ is not continuous, and hence $f(q, x)_x$ contains a delta function. This can be observed with the advection equation (2.1) if $u(x)$ changes sign from positive to negative at some point, so that there is inflow towards this point from both directions and hence the density must blow up at this single point. In terms of the Riemann problem, this corresponds to the case $u_{i-1} > 0$ and $u_i < 0$. All characteristics are approaching $x_{i-1/2}$, and the Riemann solution contains no propagating wave, only a delta function at $x_{i-1/2}$ together with a jump from $Q^l_{i-1/2} = Q_{i-1}$ to $Q^r_{i-1/2} = Q_i$ that in general does not satisfy (2.5). Note that in this case the standard Rankine–Hugoniot condition does not hold because of the accumulation of mass in the singularity.

For the traffic flow problem, the case $u_{i-1} > 0$ and $u_i < 0$ corresponds to two opposing one-way streets meeting at a point. While we can make physical sense of a singular solution in this case, it is not a reasonable model of reality. To more properly model this situation we should use a nonlinear traffic model in which the velocity depends on the density, for example, the classical flux (see [19], [31])

$$f_i(q) = u_i(1 - q)q, \tag{2.7}$$

where u_i is now the maximum speed (at $q = 0$) but the speed drops linearly to 0 as the density increases to $q = 1$ (bumper-to-bumper traffic). In this case even taking $u_{i-1} > 0$ and $u_i < 0$ gives a sensible Riemann solution in which $Q^l_{i-1/2} = Q^r_{i-1/2} = 1$ and two traffic-jam shock waves move upstream in each direction. In this case there

are *two* propagating waves in the Riemann solution even though $m = 1$. This is another way in which the Riemann solution can become more complicated in the case in which eigenvalues change sign.

Now consider a variable-coefficient linear system of m equations of the form

$$q_t + (A(x)q)_x = 0. \tag{2.8}$$

A cell-centered discretization leads to a matrix A_i associated with cell i. Suppose that this matrix is nonsingular, with $\mathcal{P}_i$ positive eigenvalues and $m - \mathcal{P}_i$ negative eigenvalues. The generalized Riemann solution must now satisfy the equations

$$\begin{cases} q_t + A_{i-1}q_x = 0 & \text{if } x < x_{i-1/2}, \\ q_t + A_i q_x = 0 & \text{if } x > x_{i-1/2}, \end{cases} \tag{2.9}$$

with data (1.4). This has a bounded solution, provided that $\mathcal{P}_{i-1} = \mathcal{P}_i \equiv \mathcal{P}$ and that the set of m vectors obtained by taking the eigenvectors of A_{i-1} that correspond to negative eigenvalues along with the eigenvectors of A_i that correspond to positive eigenvalues forms a linearly independent set. These are the vectors we use as the $r^p_{i-1/2}$ for $p = 1, 2, \ldots, m$, along with the corresponding eigenvalues as the $s^p_{i-1/2}$. Then the Riemann problem has a unique solution of the form illustrated in Figure 1(b), with m propagating waves proportional to these vectors. The left-going $m - \mathcal{P}$ waves satisfy the Rankine–Hugoniot conditions for the equation $q_t + A_{i-1}q_x = 0$ valid for $x < x_{i-1/2}$, while the right-going $\mathcal{P}$ waves satisfy the Rankine–Hugoniot conditions for the equation $q_t + A_i q_x = 0$ valid for $x > x_{i-1/2}$.

At $x_{i-1/2}$, the values $Q^l_{i-1/2}$ and $Q^r_{i-1/2}$ must be related via $A_{i-1}Q^l_{i-1/2} = A_i Q^r_{i-1/2}$ so that the flux is continuous. In the linear case, this condition can be used to determine the waves $\mathcal{W}^p_{i-1/2}$ as follows. We want to find wave strengths $\alpha^p_{i-1/2}$ so that

$$Q^l_{i-1/2} = Q_{i-1} + \sum_{p=1}^{m-\mathcal{P}} \alpha^p_{i-1/2} r^p_{i-1/2} \tag{2.10}$$

and

$$Q^r_{i-1/2} = Q_i - \sum_{p=m-\mathcal{P}+1}^{m} \alpha^p_{i-1/2} r^p_{i-1/2}, \tag{2.11}$$

and we also need $A_{i-1}Q^l_{i-1/2} = A_i Q^r_{i-1/2}$ to be satisfied, which requires

$$A_{i-1}\left[Q_{i-1} + \sum_{p=1}^{m-\mathcal{P}} \alpha^p_{i-1/2} r^p_{i-1/2}\right] = A_i\left[Q_i - \sum_{p=m-\mathcal{P}+1}^{m} \alpha^p_{i-1/2} r^p_{i-1/2}\right]. \tag{2.12}$$

Rearranging this leads to

$$A_i Q_i - A_{i-1}Q_{i-1} = \sum_{p=1}^{m} \alpha^p_{i-1/2} s^p_{i-1/2} r^p_{i-1/2}. \tag{2.13}$$

Again we see that it is the flux difference $f_i(Q_i) - f_{i-1}(Q_{i-1})$ that should be decomposed into eigenvectors, rather than the Q difference.

In this paper we concentrate on problems in which the number of positive eigenvalues of $A(x)$, or more generally of the flux Jacobian $f_q(q,x)$, does not vary with x. Of course many interesting problems involve "sonic points" where the eigenvalues pass through zero. In some cases this leads to singular solutions, as discussed above for the advection equation. Even in cases where there is a bounded weak solution, it is necessary to impose appropriate admissibility conditions to select the physically correct solution, and this can be more subtle than in the autonomous case. For some discussions of such problems, see, for example, [5, 6, 9, 10, 12, 15, 17, 25, 26]. We are continuing to study extensions of our algorithm to particular problems of this form.

3. The wave-propagation algorithms. We first briefly summarize the wave-propagation algorithm described in [20], which should be consulted for more details and explanation. This method can be applied to any hyperbolic system for which waves $\mathcal{W}^p_{i-1/2}$ and speeds $s^p_{i-1/2}$ can be defined, and can also be applied to spatially varying flux functions, provided that the Riemann solution can be obtained. One way to obtain these waves is to first compute $\mathcal{Z}^p_{i-1/2}$ and then divide by $s^p_{i-1/2}$, although we show later in this section that this division is not necessary. The first-order version corresponds to Godunov's method but is written in terms of the waves and their influence on the cell averages (1.3) rather than using interface fluxes as in (1.6). The standard wave-propagation algorithm has the form

$$Q_i^{n+1} = Q_i^n - \frac{\Delta t}{\Delta x}[\mathcal{A}^+\Delta Q_{i-1/2} + \mathcal{A}^-\Delta Q_{i+1/2}], \tag{3.1}$$

where

$$\mathcal{A}^+\Delta Q_{i-1/2} = \sum_{p=1}^{m} (s^p_{i-1/2})^+ \mathcal{W}^p_{i-1/2} \tag{3.2}$$

and

$$\mathcal{A}^-\Delta Q_{i+1/2} = \sum_{p=1}^{m} (s^p_{i+1/2})^- \mathcal{W}^p_{i+1/2}. \tag{3.3}$$

Here $s^+ = \max(s,0)$ and $s^- = \min(s,0)$. The "fluctuations" $\mathcal{A}^+\Delta Q_{i-1/2}$ and $\mathcal{A}^-\Delta Q_{i+1/2}$ model the contribution to the cell average Q_i due to right-going waves from $x_{i-1/2}$ and left-going waves from $x_{i+1/2}$, respectively. This algorithm is extended to a high-resolution version by adding in correction fluxes:

$$Q_i^{n+1} = Q_i^n - \frac{\Delta t}{\Delta x}[\mathcal{A}^+\Delta Q_{i-1/2} + \mathcal{A}^-\Delta Q_{i+1/2}] - \frac{\Delta t}{\Delta x}[\tilde{F}_{i+1/2} - \tilde{F}_{i-1/2}], \tag{3.4}$$

where

$$\tilde{F}_{i-1/2} = \frac{1}{2}\sum_{p=1}^{m} |s^p_{i-1/2}| \left(1 - \frac{\Delta t}{\Delta x}|s^p_{i-1/2}|\right) \widetilde{\mathcal{W}}^p_{i-1/2}. \tag{3.5}$$

Here $\widetilde{\mathcal{W}}^p_{i-1/2}$ is a limited version of the wave $\mathcal{W}^p_{i-1/2}$ obtained by comparing $\mathcal{W}^p_{i-1/2}$ to $\mathcal{W}^p_{I-1/2}$, the corresponding wave from the adjacent Riemann problem on the upwind side, where

$$I = \begin{cases} i-1 & \text{if } s^p_{i-1/2} > 0, \\ i+1 & \text{if } s^p_{i-1/2} < 0. \end{cases} \tag{3.6}$$

If no limiter is applied ($\widetilde{\mathcal{W}}^p_{i-1/2} = \mathcal{W}^p_{i-1/2}$), then for a linear problem this algorithm reduces to the Lax–Wendroff method. It can be shown to be second-order accurate more generally for smooth solutions to nonlinear problems, as we verify below even in the case of a spatially varying flux function. The use of a limiter (as described further in [20]) reduces nonphysical oscillations and yields a robust algorithm for computing shocks and other discontinuous solutions.

The above formulas are easily modified to use the f-waves $\mathcal{Z}^p_{i-1/2}$ directly in place of the $\mathcal{W}^p_{i-1/2}$. Since each $\mathcal{Z}^p_{i-1/2}$ corresponds to $s^p_{i-1/2}\mathcal{W}^p_{i-1/2}$, we simply replace (3.2), (3.3) by

$$\begin{aligned} \mathcal{A}^-\Delta Q_{i-1/2} &= \sum_{p:s^p_{i-1/2}<0} \mathcal{Z}^p_{i-1/2}, \\ \mathcal{A}^+\Delta Q_{i-1/2} &= \sum_{p:s^p_{i-1/2}>0} \mathcal{Z}^p_{i-1/2}, \end{aligned} \tag{3.7}$$

where we sum only over the p for which $s^p_{i-1/2}$ is negative or positive. We replace the correction flux (3.5) by

$$\tilde{F}_{i-1/2} = \frac{1}{2}\sum_{p=1}^{M_w} \operatorname{sgn}(s^p_{i-1/2}) \left(1 - \frac{\Delta t}{\Delta x}|s^p_{i-1/2}|\right) \widetilde{\mathcal{Z}}^p_{i-1/2}. \tag{3.8}$$

Now $\widetilde{\mathcal{Z}}^p$ is a limited version of the f-wave $\mathcal{Z}^p$ obtained in the same manner as $\widetilde{\mathcal{W}}^p$ would be obtained from $\mathcal{W}^p$.

The standard wave-propagation algorithm is implemented in the CLAWPACK software [18], and this can be applied to the problems considered here by defining $\mathcal{W}^p = \mathcal{Z}^p/s^p$, since we assume $s^p \neq 0$. However, the modification just described appears more robust since we do not need to worry about the case in which s^p is close to zero. Note that when limiters are used, the two approaches are not identical if the wave speeds $s^p_{i-1/2}$ are spatially varying, since these values come into the $\mathcal{Z}^p_{i-1/2}$. If some $s^p_{i-1/2}$ is close to zero, then the resulting $\mathcal{W}^p_{i-1/2}$ may be very large, resulting in a nonphysical limiting of the neighboring waves that can be avoided by working directly in terms of the $\mathcal{Z}^p_{i-1/2}$. The f-wave approach has also been implemented in CLAWPACK with a minor change in the code, as described at http://www.amath.washington.edu/~claw/fwave.html.

When no limiter is applied, the method is second-order accurate for conservation laws with spatially varying fluxes, provided that the variation of the flux $f(q, x)$ is smooth in x along with the desired solution $q(x, t)$. To obtain this second-order accuracy we must assume that the Riemann solver being used is consistent with the flux function in a suitable manner. For the proof we compute the local truncation error and so take a pointwise approach where $Q^n_i \approx q(x_i, t_n)$. For the Riemann problem between Q_{i-1} and Q_i we assume that the flux difference $f(Q_i, x_i) - f(Q_{i-1}, x_{i-1})$ is decomposed into waves $\mathcal{Z}^p_{i-1/2}$,

$$f(Q_i, x_i) - f(Q_{i-1}, x_{i-1}) = \sum_{p=1}^{m} \mathcal{Z}^p_{i-1/2}. \tag{3.9}$$

We assume that these are proportional to eigenvectors $r^p_{i-1/2}$ of some matrix $A_{i-1/2} = A(Q_{i-1}, x_{i-1}, Q_i, x_i)$, where the matrix-valued function A approximates the Jacobian

matrix $f_q(q,x)$ to sufficient accuracy. Specifically we suppose that

$$A(q(x-\Delta x),x-\Delta x,q(x),x) = f_q\left(q\left(x-\frac{\Delta x}{2}\right),x-\frac{\Delta x}{2}\right)+E(x,\Delta x), \tag{3.10}$$

where the error $E(x,\Delta x)$ satisfies

$$E(x,\Delta x)=\mathcal{O}(\Delta x) \quad \text{as } \Delta x\to 0 \tag{3.11}$$

and

$$\frac{E(x,\Delta x)-E(x-\Delta x,\Delta x)}{\Delta x}=\mathcal{O}(\Delta x) \quad \text{as } \Delta x\to 0. \tag{3.12}$$

These conditions require that A approximate the Jacobian matrix to only $\mathcal{O}(\Delta x)$, but also that the error be smoothly varying with x. Any reasonable choice of A will work, as long as we are consistent from one point to the next. Thus we could take $A_{i-1/2}=f'_{i-1}(Q_{i-1})$ or $A_{i-1/2}=f'_i(Q_i)$, as long as we consistently choose one or the other for all i. The choice advocated in section 2, selecting some eigencomponents from each Jacobian, also yields a consistent approximation.

To verify the second-order accuracy of a method satisfying this consistency condition, we write out the updating formula (3.4) for Q_i^{n+1} using the fluctuations (3.7) and the corrections (3.8). This gives

$$\begin{aligned}
Q_i^{n+1} &= Q_i^n - \frac{\Delta t}{\Delta x}\left[\sum_{p:s^p_{i-1/2}>0}\mathcal{Z}^p_{i-1/2}+\sum_{p:s^p_{i-1/2}<0}\mathcal{Z}^p_{i+1/2}\right]\\
&\quad -\frac{\Delta t}{2\Delta x}\left[\sum_{p=1}^m \operatorname{sgn}(s^p_{i+1/2})\left(1-\frac{\Delta t}{\Delta x}|s^p_{i+1/2}|\right)\mathcal{Z}^p_{i+1/2}\right.\\
&\qquad \left.-\sum_{p=1}^m \operatorname{sgn}(s^p_{i-1/2})\left(1-\frac{\Delta t}{\Delta x}|s^p_{i-1/2}|\right)\mathcal{Z}^p_{i-1/2}\right]\\
&= Q_i^n - \frac{\Delta t}{2\Delta x}\left[\sum_{p=1}^m \mathcal{Z}^p_{i-1/2}+\sum_{p=1}^m \mathcal{Z}^p_{i+1/2}\right]\\
&\quad +\frac{\Delta t^2}{2\Delta x^2}\left[\sum_{p=1}^m s^p_{i+1/2}\mathcal{Z}^p_{i+1/2}-\sum_{p=1}^m s^p_{i-1/2}\mathcal{Z}^p_{i-1/2}\right]\\
&= Q_i^n - \frac{\Delta t}{2\Delta x}\left[\sum_{p=1}^m \mathcal{Z}^p_{i-1/2}+\sum_{p=1}^m \mathcal{Z}^p_{i+1/2}\right]\\
&\quad +\frac{\Delta t^2}{2\Delta x^2}\left[A_{i+1/2}\sum_{p=1}^m \mathcal{Z}^p_{i+1/2}-A_{i-1/2}\sum_{p=1}^m \mathcal{Z}^p_{i-1/2}\right].
\end{aligned} \tag{3.13}$$

To obtain the last line, we have used the fact that each $\mathcal{Z}^p$ is an eigenvector of the corresponding A with eigenvalue s^p. We can now use the assumption (3.9) to rewrite

this as

$$
\begin{aligned}
Q_i^{n+1} = Q_i^n &- \frac{\Delta t}{2\Delta x}(f(Q_{i+1}, x_{i+1}) - f(Q_{i-1}, x_{i-1})) \\
&+ \frac{\Delta t^2}{2\Delta x^2}\left[A_{i+1/2}(f(Q_{i+1}, x_{i+1}) - f(Q_i, x_i))\right. \\
&\qquad \left. - A_{i-1/2}(f(Q_i, x_i) - f(Q_{i-1}, x_{i-1}))\right].
\end{aligned} \tag{3.14}
$$

This agrees with the Taylor series expansion of the true solution, to sufficient accuracy that a standard computation of the truncation error now shows that the method is second-order accurate, provided that A is a consistent approximation to $f_q(q, x)$ as described above. To develop the Taylor series we note that

$$
\begin{aligned}
q_t &= -f(q, x)_x, \\
q_{tt} &= -\big(f_q(q, x)q_t\big)_x = \big[f_q(q, x)f(q, x)_x\big]_x,
\end{aligned} \tag{3.15}
$$

and so

$$
q(x_i, t_{n+1}) = q(x_i, t_n) - \Delta t f(q)_x + \frac{1}{2}\Delta t^2\big[f_q(q, x)f(q, x)_x\big]_x + \mathcal{O}(\Delta t^3), \tag{3.16}
$$

where all terms on the right are evaluated at (x_i, t_n). The $\mathcal{O}(\Delta t)$ terms in (3.16) and (3.14) agree to $\mathcal{O}(\Delta t \Delta x^2)$. The conditions (3.11) and (3.12) guarantee that

$$
\begin{aligned}
&A(q(x - \Delta x),\, q(x))\left(\frac{f(q(x), x) - f(q(x - \Delta x), x - \Delta x)}{\Delta x}\right) \\
&\quad = f_q\left(q\left(x - \frac{\Delta x}{2}\right), x - \frac{\Delta x}{2}\right)\; f\left(q\left(x - \frac{\Delta x}{2}\right), x - \frac{\Delta x}{2}\right)_x + E_2(x, \Delta x),
\end{aligned} \tag{3.17}
$$

with $E_2(x, \Delta x)$ satisfying the same conditions as $E(x, \Delta x)$. This in turn is sufficient to show that the final term in (3.14) agrees with the $\mathcal{O}(\Delta t^2)$ term in (3.16) to $\mathcal{O}(\Delta t^2 \Delta x)$, as required for second-order accuracy. See [3] for another discussion of the accuracy of this algorithm in the context of a wave propagation problem in general relativity.

4. Elastic waves in heterogeneous media. As an example, we consider the propagation of compressional waves in a one-dimensional elastic rod with density $\rho(x) > 0$ and a stress-strain relation $\sigma(\epsilon, x)$ that may also vary with x and that satisfies $\sigma_\epsilon(\epsilon, x) > 0$ everywhere. The equations of motion in a Lagrangian frame (relative to a reference configuration) are then given by the conservation laws (1.1), with

$$
q(x, t) = \begin{bmatrix} \epsilon \\ \rho u \end{bmatrix} \equiv \begin{bmatrix} \epsilon \\ \mathfrak{m} \end{bmatrix}, \qquad f(q, x) = \begin{bmatrix} -\mathfrak{m}/\rho(x) \\ -\sigma(\epsilon, x) \end{bmatrix}, \tag{4.1}
$$

where $\epsilon(x, t)$ is the strain and $\mathfrak{m}(x, t) = \rho(x)u(x, t)$ is the momentum. The first equation in this system expresses the kinematic relation $\epsilon_t = u_x$, while the second equation is Newton's second law.

The Jacobian matrix for this system is

$$
f_q(q, x) = \begin{bmatrix} 0 & -1/\rho(x) \\ -\sigma_\epsilon(\epsilon, x) & 0 \end{bmatrix}, \tag{4.2}
$$

with eigenvalues $\pm c(\epsilon, x)$, where the compressional wave speed is given by

$$c(q,x) = \sqrt{\frac{\sigma_\epsilon(\epsilon,x)}{\rho(x)}}. \tag{4.3}$$

The corresponding eigenvectors are

$$r^1(q,x) = \begin{bmatrix} 1 \\ Z(q,x) \end{bmatrix} \qquad \text{for } s^1(q,x) = -c(q,x) \tag{4.4}$$

and

$$r^2(q,x) = \begin{bmatrix} 1 \\ -Z(q,x) \end{bmatrix} \qquad \text{for } s^2(q,x) = c(q,x), \tag{4.5}$$

where $Z(q,x) = \rho(x)c(q,x)$ is the impedance. For this system of two equations there is always one negative eigenvalue and one positive eigenvalue at every point, corresponding to waves propagating to the left and right, respectively, and the eigenvalues never change sign in this Lagrangian frame. We thus expect the flux to be continuous at any material discontinuity. This also follows naturally from physical considerations, since the components of flux are $-u$ and $-\sigma$. Clearly the velocity and stress must be continuous at an interface for the continuum model to hold.

This Riemann problem is discussed further in [22], where a description of an approach to computing the exact solution is described. However, an approximate Riemann solver is found to work very well, based on defining the matrix $A_{i-1/2}$ in terms of its eigenvectors and eigenvalues as

$$r^1_{i-1/2} = r^1_{i-1} = \begin{bmatrix} 1 \\ Z_{i-1} \end{bmatrix}, \qquad s^1_{i-1/2} = -\sqrt{\frac{\sigma'_{i-1}(\epsilon_{i-1})}{\rho_{i-1}}}, \tag{4.6}$$

and

$$r^2_{i-1/2} = r^2_i = \begin{bmatrix} 1 \\ -Z_i \end{bmatrix}, \qquad s^2_{i-1/2} = \sqrt{\frac{\sigma'_i(\epsilon_i)}{\rho_i}}. \tag{4.7}$$

The algorithm described in section 3 can now be applied by decomposing the flux difference $f_i(Q_i) - f_{i-1}(Q_{i-1})$ as a linear combination of these eigenvectors. This algorithm has been used in [22] to solve an elastic wave propagation problem in a heterogeneous rod with rapidly varying piecewise constant properties (a layered medium or laminate). An interesting nonlinear effect was found in this case: a smooth pulse breaks up into solitary waves that appear to behave as solitons; see also [24]. Here we use this and a related example with smoothly varying material properties as a test of the accuracy of the numerical method. We take

$$\begin{aligned} \rho(x) &= \phi(x), \\ \sigma(\epsilon,x) &= (\epsilon\,\phi(x)) + 0.3\,(\epsilon\,\phi(x))^2 \end{aligned} \tag{4.8}$$

for some function $\phi(x)$, with initial data

$$u(x,0) = \epsilon(x,0) = 0 \tag{4.9}$$

and boundary conditions

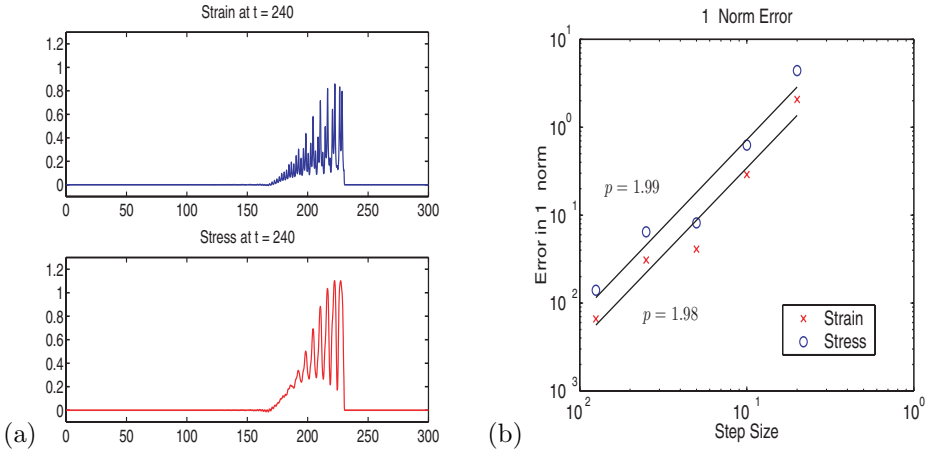

FIG. 2. *A nonlinear elasticity example in a rapidly varying continuous medium. Plots indicate* (a) *the stress and strain on a grid with* 3000 *points and* (b) *the estimated order of accuracy for grid resolutions of* $1500 \times 2^{n-1}$ *for* $n = 1, \ldots, 5$.

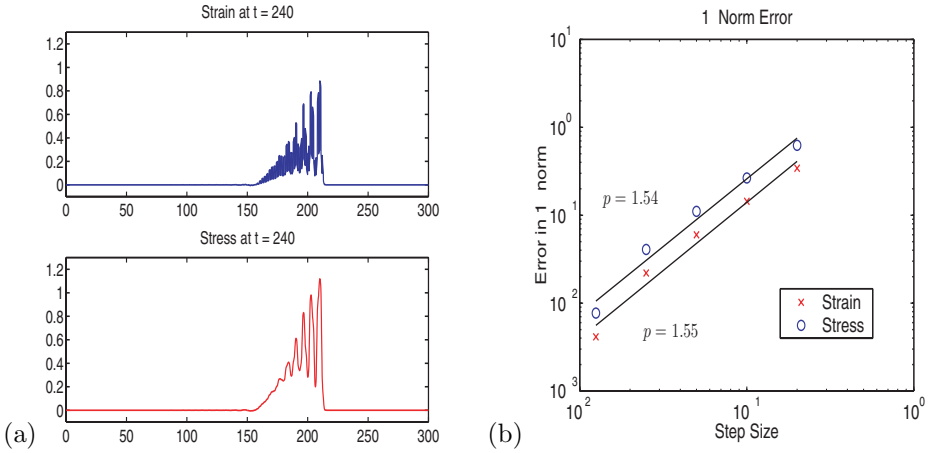

FIG. 3. *A nonlinear elasticity example in a rapidly varying discontinuous medium. Plots indicate* (a) *the stress and strain on a grid with* 3000 *points and* (b) *the estimated order of accuracy for grid resolutions of* $1500 \times 2^{n-1}$ *for* $n = 1, \ldots, 5$.

$$u(0,t) = \begin{cases} -\frac{2}{10}(1 + \cos(\frac{\pi}{30}(t-30))) & \text{if} \quad t \le 60, \\ 0 & \text{if} \quad t > 60. \end{cases} \tag{4.10}$$

These boundary conditions generate a smooth incoming pulse from the left boundary. Figures 2(a) and 3(a) show this pulse at a later time in two cases where the material parameters are rapidly varying relative to the width of the pulse, leading to the development of dispersive oscillations (see [22]). In the test of Figure 2, the material parameters vary smoothly,

$$\phi(x) = 2 - \sin(\pi x), \tag{4.11}$$

and a mesh refinement study shows that second-order accuracy is achieved (see Figure

2(b)). Figure 3 shows a case in which the material parameters are discontinuous,

$$\phi(x) = \begin{cases} 1 & \text{if} \quad 2j < x < 2j+1, \\ 3 & \text{if} \quad 2j+1 < x < 2j+2. \end{cases} \tag{4.12}$$

In this case we do not expect to achieve second-order accuracy, but we still observe a convergence rate of about 1.5 in both the stress (which is continuous) and the strain (which is discontinuous at each discontinuity in $\phi(x)$).

5. Linear acoustics. The equations for linear acoustics can be obtained from the elasticity problem above if the stress-strain relation is linear,

$$\sigma(\epsilon, x) = K(x)\epsilon, \tag{5.1}$$

where $K(x)$ is the bulk modulus of compressibility. The elasticity system then has the form (2.8) with q as in (4.1) and

$$A(x) = \begin{bmatrix} 0 & -1/\rho(x) \\ K(x) & 0 \end{bmatrix}. \tag{5.2}$$

The eigenvalues are $\pm c(x)$, where the sound speed is $c(x) = \sqrt{K(x)/\rho(x)}$. The eigenvectors are still given by (4.4) and (4.5), although in this case the impedance $Z(x) = \rho(x)c(x)$ and the eigenvectors depend only on x. The procedure described in the previous section produces the exact Riemann solution in this case. The wave-propagation algorithm based on f-waves can be used to solve this variable-coefficient linear system, which remains in conservation form.

Alternatively, the acoustics equations can be written in a more familiar form if we introduce the pressure $p = -\sigma = -K\epsilon$ so that the above system becomes

$$\frac{\partial}{\partial t}\begin{bmatrix} p/K(x) \\ \rho(x)u \end{bmatrix} + \frac{\partial}{\partial x}\begin{bmatrix} u \\ p \end{bmatrix} = 0. \tag{5.3}$$

This can be rewritten as a nonconservative variable-coefficient hyperbolic system as

$$\frac{\partial}{\partial t}\begin{bmatrix} p \\ u \end{bmatrix} + \begin{bmatrix} 0 & K(x) \\ 1/\rho(x) & 0 \end{bmatrix}\frac{\partial}{\partial x}\begin{bmatrix} p \\ u \end{bmatrix} = 0. \tag{5.4}$$

The wave-propagation algorithms have been extended to apply to nonconservative hyperbolic systems in [20], where the acoustics system (5.4) is used as an example. These algorithms are further studied in [7], where it is observed that good results are obtained even when the coefficients $K(x)$ and $\rho(x)$ are rapidly varying and/or discontinuous. However, the conservative form based on (4.1) has advantages, at least for smooth solutions, since the method proposed here will give a fully second-order accurate method, while the previous approach based on (5.4) is formally only first-order accurate (although the results are still "high resolution" in the sense discussed in section 2.4 of [20], and much better than classical first-order methods would give).

To illustrate this improvement, both the nonconservative and the new conservative algorithm are tested on three different acoustics problems of increasing complexity. In each case the initial conditions are given by

$$\begin{aligned} p(x,0) &= \begin{cases} \frac{7}{4} - \frac{3}{4}\cos\bigl(10\,\pi\,x - 4\,\pi\bigr) & \text{if} \quad 0.4 < x < 0.6, \\ 1 & \text{otherwise}, \end{cases} \\ u(x,0) &= 0, \end{aligned} \tag{5.5}$$

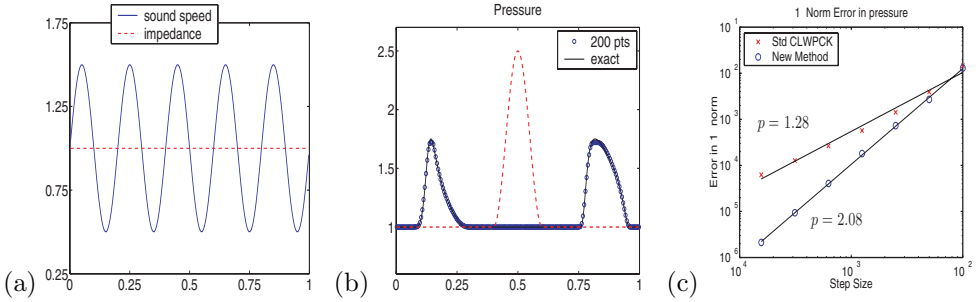

FIG. 4. *Linear acoustics example with variation in only the eigenvalues. Shown are* (a) *the impedance and the sound speed;* (b) *the solution at time* $t = 0$ *(dashed line) and* $t = 0.3$ *(circles) on a grid with* 200 *points, along with the "exact" solution at* $t = 0.3$ *(solid line); and* (c) *the order of accuracy in the* 1*-norm for both the standard* CLAWPACK *(nonconservative) approach and the new method.*

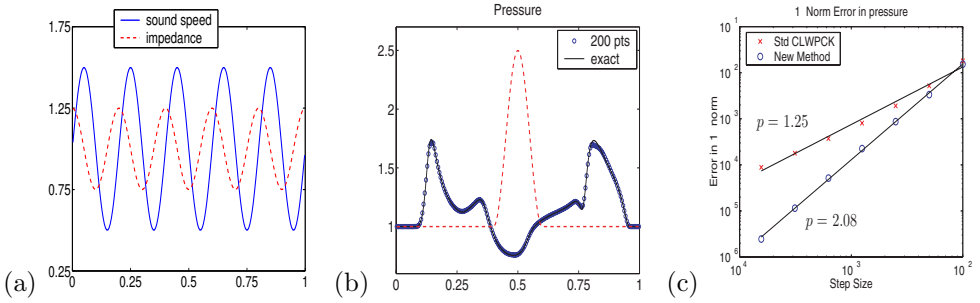

FIG. 5. *Linear acoustics example with variation in both the eigenvalues and the eigenvectors. Shown are* (a) *the impedance and the sound speed;* (b) *the solution at time* $t = 0$ *(dashed line) and* $t = 0.35$ *(circles) on a grid with* 200 *points, along with the "exact" solution at* $t = 0.35$ *(solid line); and* (c) *the order of accuracy in the* 1*-norm for both the standard* CLAWPACK *(nonconservative) approach and the new method.*

and an "exact" reference solution is computed with the conservative scheme on a grid with 20,000 points.

In Figure 4 we apply both wave-propagation methods to a problem where the eigenvalues are spatially varying but the eigenvectors are identically constant, with

$$c(x) = 1 + 0.5\sin(10\pi x), \qquad Z(x) = 1. \tag{5.6}$$

The linear system can then be diagonalized and reduced to two variable-coefficient advection equations. Hence left-going and right-going waves are decoupled, and the initial pulse splits into two distinct waves as seen in the figure.

In Figure 5 we consider a case in which the impedance and hence the eigenvectors are also spatially varying:

$$c(x) = 1 + 0.5\sin(10\pi x), \qquad Z(x) = 1 + 0.25\cos(10\pi x). \tag{5.7}$$

Now the left-going and right-going waves are fully coupled.

In both of these cases the algorithm proposed here produces second-order accurate results. The observed order is roughly 2.08 in each case, as shown in Figures 4(c) and 5(c). These plots also show that the nonconservative method is formally only first-order accurate.

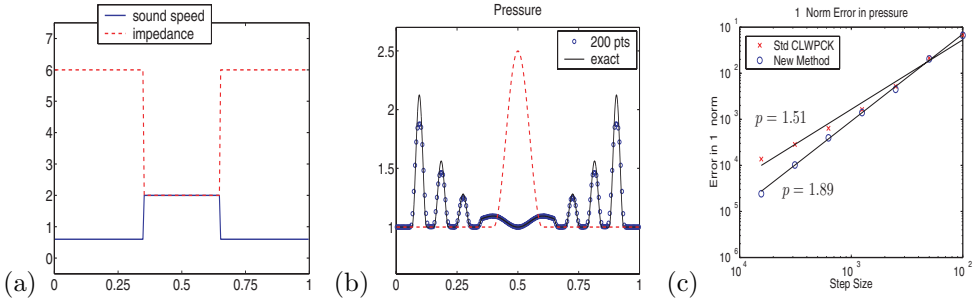

FIG. 6. *Linear acoustics example with a jump discontinuity in both the eigenvalues and the eigenvectors. Shown are* (a) *the impedance and the sound speed;* (b) *the solution at time* $t = 0$ *(dashed line) and* $t = 0.5$ *(circles) on a grid with* 200 *points, along with the "exact" solution at* $t = 0.5$ *(solid line); and* (c) *the order of accuracy in the* 1*-norm for both the standard* CLAWPACK *(nonconservative) approach and the new method.*

In Figure 6 we consider a problem where the medium is discontinuous:

$$c(x) = \begin{cases} 0.6 & \text{if} \quad 0.35 < x < 0.65, \\ 2 & \text{otherwise,} \end{cases} \qquad Z(x) = \begin{cases} 6 & \text{if} \quad 0.35 < x < 0.65, \\ 2 & \text{otherwise.} \end{cases} \tag{5.8}$$

The initial pulse splits into waves moving to the left and right that repeatedly reflect off the interfaces, leading to a train of waves moving in each direction. In this case we do not expect second-order accuracy but achieve a rate of 1.89 with the f-wave approach, whereas the nonconservative algorithm shows a lower rate that appears to deteriorate further as the grid is refined.

6. Extension to higher dimensions. The wave-propagation algorithm developed in section 3 is easily extended to multidimensional conservation laws following the same procedure used in [20] for the standard algorithm. (See [16] for the three-dimensional extension.) In two space dimensions a conservation law with spatially varying fluxes takes the form

$$q_t + f(q, x, y)_x + g(q, x, y)_y = 0, \tag{6.1}$$

where $q = q(x, y, t)$. The two-dimensional wave-propagation algorithm is based on solving one-dimensional Riemann problems normal to each cell edge, and the f-wave approach developed here can again be used in place of the usual wave decomposition. At the interface between cells $(i-1, j)$ and (i, j), for example, the flux difference $f_{ij}(Q_{ij}) - f_{i-1,j}(Q_{i-1,j})$ is split into a left-going portion $\mathcal{A}^- \Delta Q_{i-1/2,j}$ and a right-going portion $\mathcal{A}^+ \Delta Q_{i-1/2,j}$. In addition to the second-order correction terms described in section 3, it is also necessary to compute transverse correction terms obtained by splitting these fluctuations into eigenvectors of approximations to the transverse Jacobian g_q at interfaces above and below the neighboring cells. These eigenvectors will be available from the Riemann solution procedure in the y-direction and can be applied directly.

As an example, we consider the two-dimensional acoustics equations as a generalization of the tests in the previous section. This linear system has the form (6.1) with

$$q = \begin{bmatrix} q^1 \\ q^2 \\ q^3 \end{bmatrix} = \begin{bmatrix} \epsilon \\ \rho u \\ \rho v \end{bmatrix},$$

and

$$f(q,x,y) = \begin{bmatrix} -q^2/\rho(x,y) \\ K(x,y)q^1 \\ 0 \end{bmatrix}, \qquad g(q,x,y) = \begin{bmatrix} -q^3/\rho(x,y) \\ 0 \\ K(x,y)q^1 \end{bmatrix}.$$

Alternatively this can be written as a nonconservative system in terms of the pressure $p = -K(x,y)q^1$ and velocities u and v, as discussed in [20] in the context of standard wave-propagation algorithms. Here we compare the two approaches on one test problem to show that the conservative approach gives full second-order accuracy. We consider a radially symmetric problem so that a reference solution can be computed by solving a one-dimensional acoustic problem with geometric source term. As data we take

$$\begin{aligned} p(r,0) &= \begin{cases} -2\left(\frac{r-0.5}{0.18}\right)^6 + 6\left(\frac{r-0.5}{0.18}\right)^4 - 6\left(\frac{r-0.5}{0.18}\right)^2 + 2 & \text{if} \quad |r-0.5| < 0.18, \\ 0 & \text{otherwise}, \end{cases} \\ u(r,0) &= v(r,0) = 0, \\ c(r) &= Z(r) = \begin{cases} 0.175 & \text{if} \quad r \le 0.15, \\ p_1(r) & \text{if} \quad 0.15 \le r \le 0.41, \\ 0.35 & \text{if} \quad 0.41 \le r \le 0.59, \\ p_2(r) & \text{if} \quad 0.59 \le r \le 0.85, \\ 0.275 & \text{if} \quad 0.85 \le r, \end{cases} \end{aligned} \tag{6.2}$$

where $r = \sqrt{x^2+y^2}$ is the radius and $p_1(r)$ and $p_2(r)$ are polynomials that smoothly connect the surrounding piecewise constant regions.

The results shown in Figure 7 illustrate the improved accuracy achieved with the conservative algorithm.

7. Source terms and balance laws. The balance law

$$q_t + f(q,x)_x = \psi(q,x) \tag{7.1}$$

consists of a conservation law with a source term on the right-hand side. Many approaches have been studied for equations of this form, primarily in the case of an autonomous flux function $f(q)$ (e.g., [4, 8, 11, 13, 14, 28, 30]). One simple approach that is often used is the fractional step method, in which one alternates between solving the homogeneous equation (1.1) and the ordinary differential equation

$$q_t = \psi(q,x). \tag{7.2}$$

However, this may not work well when the solution is close to a steady state and $f(q,x)_x \approx \psi(q,x)$ while each term separately is large. Solving each of the equations (1.1) and (7.2) will then cause large changes in the solution, which numerically may not cancel out properly. Instead we would like to develop a wave-propagation method in which the waves model only the information that should propagate relative to the background steady state solution. One approach was proposed in [21], but we now believe that a better approach is suggested by the f-wave algorithm presented above, even in the autonomous case, and has the additional advantage of applying also with spatially varying flux functions.

We assume that the source term at time t_n can be discretized to yield values $\Psi^n_{i-1/2}$ at cell edges, and as usual we suppress the superscript n. This has the effect

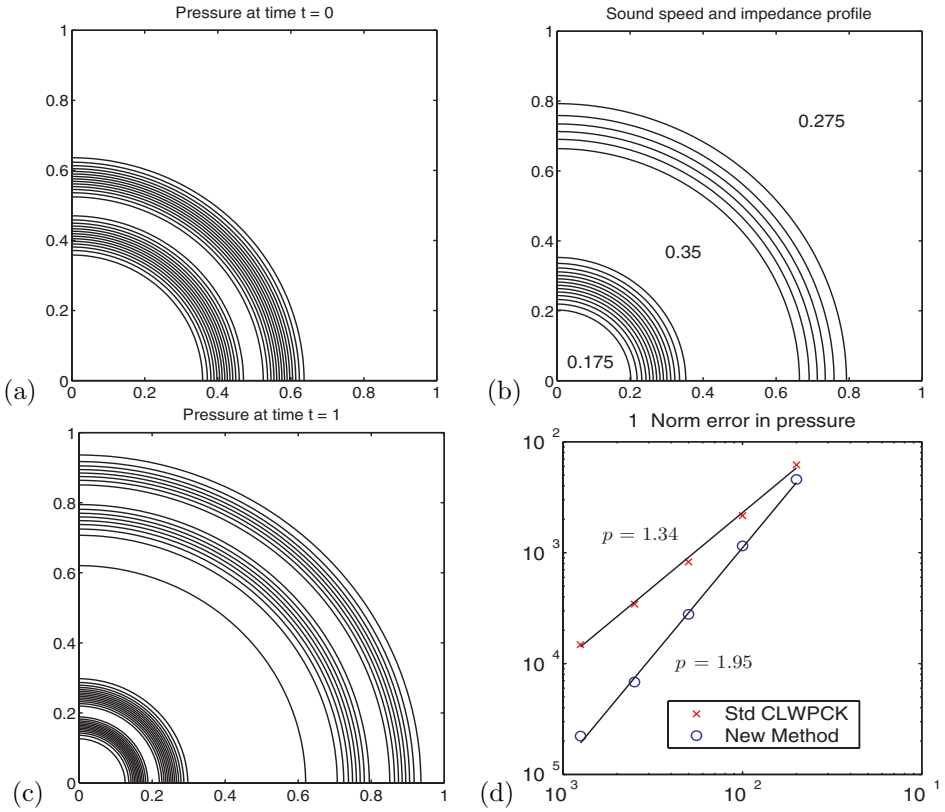

FIG. 7. *An example of linear acoustics in two dimensions. Shown are* (a) *the initial pressure distribution,* (b) *the sound speed and impedance profiles,* (c) *the solution at the final time, and* (d) *an estimate for the order of accuracy.*

of replacing the source term $\psi(q,x)$ by a function $\Psi(q,x)$ that is a sum of delta-function sources at these discrete points,

$$\Psi(q,x) = \Delta x \sum_i \Psi_{i-1/2}\, \delta(x - x_{i-1/2}). \tag{7.3}$$

Then the Riemann problem at $x_{i-1/2}$ is for the problem

$$q_t + F_{i-1/2}(q)_x = \Delta x \Psi_{i-1/2} \delta(x - x_{i-1/2}), \tag{7.4}$$

with $F_{i-1/2}(q)$ given by (1.8). The Riemann solution will still have the basic structure shown in Figure 1(b), but the delta-function source at the point $x_{i-1/2}$ leads us to expect that the flux will no longer be continuous at this point, but rather will satisfy

$$f_i(Q^r_{i-1/2}) - f_{i-1}(Q^l_{i-1/2}) = \Delta x \Psi_{i-1/2}. \tag{7.5}$$

This suggests that the f-waves $\mathcal{Z}^p_{i-1/2}$ should be based on an eigendecomposition of the form (1.17),

$$f_i(Q_i) - f_{i-1}(Q_{i-1}) - \Delta x \Psi_{i-1/2} = \sum_{p=1}^m \beta^p_{i-1/2} r^p_{i-1/2} \equiv \sum_{p=1}^m \mathcal{Z}^p_{i-1/2}. \tag{7.6}$$

The wave-propagation method of section 3 can then be applied directly.

The wave decomposition (7.6) has the effect of splitting the source term $\Psi_{i-1/2}$ into eigenvectors of an approximate Jacobian along with the flux difference. In the Godunov updates, the eigencomponents of the source term are thus distributed to the neighboring cells based on the sign of the corresponding eigenvalues. This approach to handling source terms has long been advocated (see, e.g., [28]), but we believe something new is gained by splitting the combination (7.6) as a single entity and using the resulting waves in a wave-propagation algorithm, where these waves can also be used directly in high-resolution correction terms. The method is particularly attractive in cases where the solution is close to a steady state in which $f(q,x)_x \approx \psi(q,x)$. Note that if

$$\frac{f_i(Q_i) - f_{i-1}(Q_{i-1})}{\Delta x} = \Psi_{i-1/2}, \tag{7.7}$$

then the left-hand side of (7.6) will be zero, and hence all the f-waves will have zero strength. This indicates that a numerical steady state satisfying (7.7) will be exactly maintained. If the solution is near a steady state, then it is only the deviation from steady state that is split into waves, and the correction terms (3.5) used to obtain a high-resolution method are based directly on these waves, or on limited versions of these waves.

The wave-propagation method of section 3 using the waves defined by (7.6) has been found to give good results for several test problems. It is not, however, formally second-order accurate. Even better results can be obtained if an additional term is added. A Taylor series expansion of the true solution for (7.1) requires

$$q_t = -f(q,x)_x + \psi(q,x) \tag{7.8}$$

and

$$\begin{aligned} q_{tt} &= [-f(q,x)_x + \psi(q,x)]_t \\ &= -[f_q(q,x)q_t]_x + \psi_q(q,x)q_t \\ &= [f_q(q,x)(f(q,x)_x - \psi(q,x))]_x - \psi_q(q,x)(f(q,x)_x - \psi(q,x)). \end{aligned} \tag{7.9}$$

An analysis of the wave-propagation algorithm based on the splitting (7.6), following the analysis of (3.13), shows that all terms in the Taylor series up to $\mathcal{O}(\Delta t^2)$ are modeled to sufficient accuracy *except* the final term in (7.9),

$$-\psi_q(q,x)(f(q,x)_x - \psi(q,x)), \tag{7.10}$$

involving the Jacobian matrix of the source term, ψ_q. In order to make the method fully second-order accurate, we can update Q_i^{n+1} by an additional correction of the form

$$-\frac{\Delta t^2}{2\Delta x}\psi_q(Q_i,x_i)\sum_{p=1}^{m}\frac{1}{2}(\mathcal{Z}_{i-1/2}^p + \mathcal{Z}_{i+1/2}^p). \tag{7.11}$$

This is motivated by noting that, by (7.6),

$$\frac{1}{\Delta x}\sum_{p=1}^{m}\mathcal{Z}_{i-1/2}^p \approx f(q,x)_x - \psi(q,x) \qquad \text{at } x_{i-1/2},$$

and we average this quantity over the two adjacent cell interfaces in order to obtain an approximation at the cell center. This is multiplied by the source Jacobian $\psi_q(Q_i, x_i)$ in the cell and by $\frac{1}{2}\Delta t^2$ since this is the proper weighting of q_{tt} in the Taylor series. Note that (7.11) vanishes if (7.7) is satisfied, so the same numerical steady state is preserved with this correction term added.

As an example, we consider the shallow water equations over bottom topography defined by some function $B(x)$. The equations are

$$\begin{aligned} h_t + (hu)_x &= 0, \\ (hu)_t + \left(hu^2 + \frac{1}{2}gh^2\right)_x &= -ghB'(x), \end{aligned} \tag{7.12}$$

where $h(x,t)$ is the fluid depth (see Figure 8(a)) and $u(x,t)$ is the horizontal velocity (assumed to be constant throughout the depth). The quantity hu is the momentum or discharge. A steady state solution with depth $h_0(x)$ and velocity $u_0(x)$ must have constant discharge (mass flux) D_0 from the first equation of (7.12). One possible steady state, corresponding to stationary fluid, is $u_0(x) \equiv 0$, $h_0(x) = \eta_0 - B(x)$, where η_0 is the constant surface level. If we introduce a small perturbation to the surface, we would like to be able to accurately compute the propagation of this perturbation. An example of this nature was used in [21] to illustrate the numerical artifacts that can arise with a classical fractional step method and the improvement obtained with the quasi-steady wave-propagation algorithm proposed there. Very similar results are obtained with the method developed above on this test problem, and these are not displayed here. The new approach has several advantages. It is easier to implement since it does not require the nonlinear iteration described in [21] to obtain values Q_i^- and Q_i^+, and it is more robust for problems that are farther away from steady state. It is also fully second-order accurate with the modification proposed above, and applies to problems with spatially varying fluxes.

To verify the accuracy of this method for a problem with both a spatially varying flux and a source term, we consider a linearized version of the shallow water equations presented above. The propagation of a small perturbation against a particular steady state can be modeled by the linear system

$$\tilde{q}_t(x,t) + (A(x)\tilde{q}(x,t))_x = \psi_q(q_0(x), x)\tilde{q}(x,t), \tag{7.13}$$

where $\tilde{q}(x,t)$ is the perturbation to the steady state $q_0(x)$ and

$$A(x) = f'(q_0(x)) = \begin{bmatrix} 0 & 1 \\ 2h_0(x) - u^2(x) & 2u_0(x) \end{bmatrix} \tag{7.14}$$

and

$$\psi_q(q_0(x), x) = \begin{bmatrix} 0 & 0 \\ -gB'(x) & 0 \end{bmatrix} \tag{7.15}$$

are the Jacobian matrices of the flux function and source term, respectively. Similar problems arise in aeroacoustics or other applications where small amplitude acoustics equations are to be solved after linearizing the Euler equations about a spatially varying steady state.

As the steady state we take steady flow over a hump, as illustrated in Figure 8(a), with $g = 1$, discharge $D_0 \equiv 0.15$ everywhere, and $h = 1$, $u = 0.15$ away from the

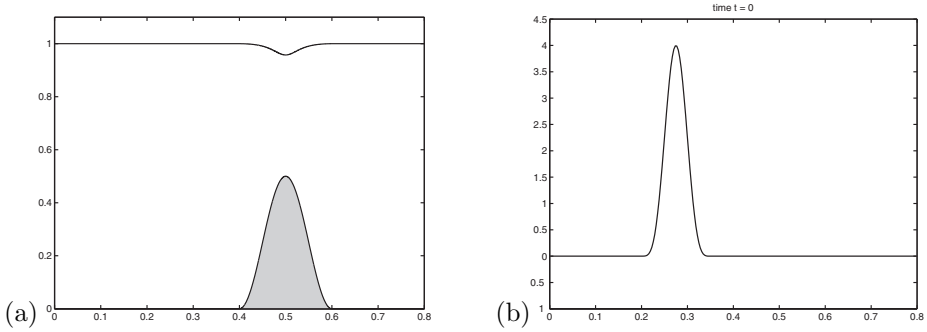

FIG. 8. (a) *Steady state depth profile for smooth subcritical flow over a hump.* (b) *Depth perturbation to the steady state solution at time* $t = 0$.

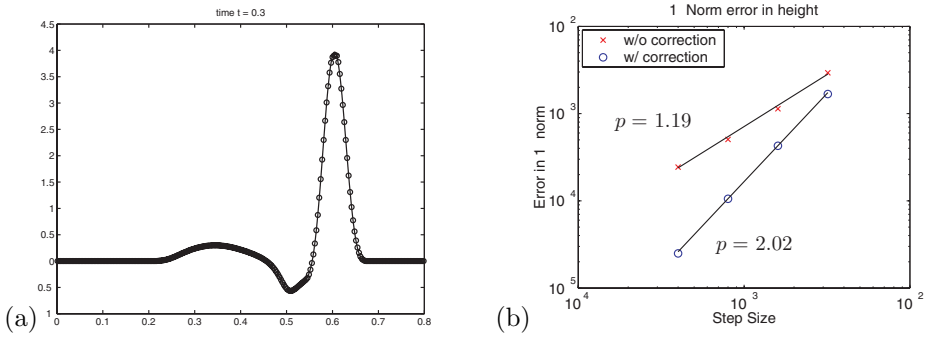

FIG. 9. (a) *Perturbation to steady state solution at time* $t = 3$*, as computed using the linearized shallow water equations. Solid line:* 8000 *grid cells. Circles:* 125 *grid cells.* (b) 1*-norm errors for the wave-propagation algorithm applied to the linearized shallow water equations for a perturbation passing through this steady state solution, as shown in Figure* 8.

hump. The steady state over the hump can be computed by solving a cubic equation at each point, using the fact that $g(h(x) + B(x)) + D^2/h^2(x)$ must be constant in x. The hump geometry is specified by

$$B(x) = \begin{cases} 0.25(\cos(\pi(x - 0.5)/0.1 + 1)) & \text{if } |x - 0.5| < 0.1, \\ 0 & \text{otherwise.} \end{cases} \tag{7.16}$$

The matrix A_i in each grid cell is computed by evaluating the Jacobian matrix (7.14) at this steady state value. The matrix $A_{i-1/2}$ used to solve the Riemann problem at interface $i - 1/2$ is then obtained by applying the standard Roe averaging procedure to the elements of A_{i-1} and A_i.

Figure 8(b) shows a smooth perturbation

$$\tilde{h}(x, 0) = \begin{cases} (1 - \cos(2\pi(x - 0.2)/0.15))^2 & \text{if } 0.2 < x < 0.35, \\ 0 & \text{otherwise,} \end{cases} \tag{7.17}$$

which is used as initial data for the linearized equations. Note that this "perturbation" is $\mathcal{O}(1)$, but for the linearized equations this can be scaled by any factor ϵ without effect on the resulting relative errors. Figure 9(a) shows the resulting solution $\tilde{h}(x, 0.3)$ after this perturbation has passed over the hump and been partially reflected. The solid line is the result computed on a fine grid with 8000 cells, while the symbols show

the result computed with 250 cells. Figure 9(b) shows a log-log plot of the error as computed in the 1-norm, using the 8000 cell solution as a reference solution. Errors are plotted for the method described above, both with and without the correction term (7.11). This term does in fact lead to fully second-order accurate results.

8. Conclusions. We have presented a general approach to developing wave-propagation algorithms for solving conservation laws with spatially varying flux functions. The key idea is to split the flux difference into eigenvectors of some approximate Jacobian matrix in order to define f-waves. This leads to formally second-order accurate methods that can be modified by limiter functions to yield high-resolution results.

This approach has several desirable features. The method is conservative and formally second-order accurate regardless of what approximate Jacobian matrix is used, provided that certain smoothness conditions are satisfied. This may be useful even for autonomous problems where a Roe average cannot easily be computed, and a simpler expression such as the arithmetic average could instead be used. (If a Roe average satisfying (1.12) is available, it is best to use it, since it has other advantages. In particular, data for which the true solution consists of a single propagating wave will yield the same structure in the approximate Riemann solution, whereas using a different approximate Jacobian may lead to more smearing.)

Another advantage of our approach is that it is not necessary to determine the jumps in the conserved variables q that typically arise across the interface in solving the Riemann problem with a spatially varying $f(q, x)$. Since the flux is assumed to be continuous across the interface, decomposition of the flux difference into eigencomponents immediately yields the propagating waves that are needed for the high-resolution wave-propagation algorithm.

Similar methods can be applied to balance laws containing source terms, as discussed in section 7. In this case a combination of the flux difference and source term is split into f-waves. An additional modification can be introduced to ensure full second-order accuracy. This method may be particularly useful in problems close to a steady state, in which case the resulting waves model only the deviation from steady state. Since these waves are used for both the first-order Godunov updates and the high-resolution correction terms, the method can exactly maintain numerical approximations to steady state and accurately compute the dynamics of small perturbations.

A number of interesting research questions remain in the case when eigenvalues of the Jacobian matrix change sign. Preliminary results indicate that our approach can also be applied to many problems of this form and yield high-resolution results, but that proper handling of such sonic points is critical. This is currently being studied in the context of some specific examples.

REFERENCES

[1] D. S. Bale, *Wave Propagation Algorithms on Curved Manifolds with Applications to Relativistic Hydrodynamics*, Ph.D. thesis, University of Washington, Seattle, WA, 2002.

[2] D. S. Bale, R. J. LeVeque, and J. A. Rossmanith, *Wave Propagation Algorithms for Hyperbolic Systems on Curved Manifolds*, in preparation.

[3] J. Bardeen and L. Buchman, *Numerical tests of evolution systems, gauge conditions, and boundary conditions for* 1*D colliding gravitational plane waves*, Phys. Rev. D, 65 (2002), article 064037.

[4] A. Bermudez and M. Vazquez, *Upwind methods for hyperbolic conservations laws with source term*, Comput. & Fluids, 23 (1994), pp. 1049–1071.

[5] F. Bouchut and F. James, *One-dimensional transport equations with discontinuous coefficients*, Nonlinear Anal., 32 (1998), pp. 891–933.
[6] S. Diehl, *A conservation law with point source and discontinuous flux function modelling continuous sedimentation*, SIAM J. Appl. Math., 56 (1996), pp. 388–419.
[7] T. Fogarty and R. J. LeVeque, *High-resolution finite volume methods for acoustics in periodic or random media*, J. Acoust. Soc. Am., 106 (1999), pp. 17–28.
[8] L. Gascón and J. M. Corberán, *Construction of second-order TVD schemes for nonhomogeneous hyperbolic conservation laws*, J. Comput. Phys., 172 (2001), pp. 261–297.
[9] T. Gimse and N. H. Risebro, *Riemann problems with a discontinuous flux function*, in Proceedings of the Third International Conference on Hyperbolic Problems, Uppsala, Sweden, B. Engquist and B. Gustafsson, eds., Studentlitteratur, 1990, pp. 488–502.
[10] T. Gimse and N. H. Risebro, *Solution of the Cauchy problem for a conservation law with a discontinuous flux function*, SIAM J. Math. Anal., 23 (1992), pp. 635–648.
[11] L. Gosse, *A well-balanced flux-vector splitting scheme designed for hyperbolic systems of conservation laws with source terms*, Comput. Math. Appl., 39 (2000), pp. 135–159.
[12] L. Gosse and F. James, *Numerical approximations of one-dimensional linear conservation equations with discontinuous coefficients*, Math. Comput., 69 (2000), pp. 987–1015.
[13] J. M. Greenberg, A. Y. LeRoux, R. Baraille, and A. Noussair, *Analysis and approximation of conservation laws with source terms*, SIAM J. Numer. Anal., 34 (1997), pp. 1980–2007.
[14] P. Jenny and B. Müller, *Rankine–Hugoniot–Riemann solver considering source terms and multidimensional effects*, J. Comput. Phys., 145 (1998), pp. 575–610.
[15] C. Klingenberg and N. H. Risebro, *Convex conservation laws with discontinuous coefficients. Existence, uniqueness and asymptotic behavior*, Comm. Partial Differential Equations, 20 (1995), pp. 1959–1990.
[16] J. O. Langseth and R. J. LeVeque, *A wave-propagation method for three-dimensional hyperbolic conservation laws*, J. Comput. Phys., 165 (2000), pp. 126–166.
[17] P. G. LeFloch and J.-C. Nedelec, *Explicit formula for weighted scalar nonlinear hyperbolic conservation laws*, Trans. Amer. Math. Soc., 308 (1988), pp. 667–683.
[18] R. J. LeVeque, Clawpack *software*, online at http://www.amath.washington.edu/~claw.
[19] R. J. LeVeque, *Numerical Methods for Conservation Laws*, Birkhäuser-Verlag, Basel, Switzerland, 1990.
[20] R. J. LeVeque, *Wave propagation algorithms for multi-dimensional hyperbolic systems*, J. Comput. Phys., 131 (1997), pp. 327–353.
[21] R. J. LeVeque, *Balancing source terms and flux gradients in high-resolution Godunov methods: The quasi-steady wave-propagation algorithm*, J. Comput. Phys., 146 (1998), pp. 346–365.
[22] R. J. LeVeque, *Finite volume methods for nonlinear elasticity in heterogeneous media*, Int. J. Numer. Meth. Fluids, 40 (2002), pp. 93–104.
[23] R. J. LeVeque and M. Pelanti, *A class of approximate Riemann solvers and their relation to relaxation schemes*, J. Comput. Phys., 172 (2001), pp. 572–591.
[24] R. J. LeVeque and D. H. Yong, *Solitary waves in layered nonlinear media*, SIAM J. Appl. Math., to appear.
[25] W. K. Lyons, *Conservation laws with sharp inhomogeneities*, Quart. Appl. Math., 40 (1983), pp. 385–393.
[26] F. Poupaud and M. Rascle, *Measure solutions to the linear multi-dimensional transport equation with non-smooth coefficients*, Comm. Partial Differential Equations, 22 (1997), pp. 337–358.
[27] P. L. Roe, *Approximate Riemann solvers, parameter vectors, and difference schemes*, J. Comput. Phys., 43 (1981), pp. 357–372.
[28] P. L. Roe, *Upwind differencing schemes for hyperbolic conservation laws with source terms*, in Nonlinear Hyperbolic Problems, C. Carraso, P.-A. Raviart, and D. Serre, eds., Lecture Notes in Math. 1270, Springer-Verlag, 1986, pp. 41–51.
[29] J. A. Rossmanith, *A Wave Propagation Method with Constrained Transport for Ideal and Shallow Water Magnetohydrodynamics*, Ph.D. thesis, University of Washington, Seattle, WA, 2002.
[30] G. Watson, D. H. Peregrine, and E. F. Toro, *Numerical solution of the shallow-water equations on a beach using the weighted average flux method*, in Computational Fluid Dynamics '92 (Brussels), C. Hirsch, J. Périaux, and W. Kordulla, eds., Elsevier Science Publishers, New York, 1992, pp. 495–502.
[31] G. Whitham, *Linear and Nonlinear Waves*, Wiley-Interscience, New York, 1974.